J Mol Model (2009) 15:1185–1191
DOI 10.1007/s00894-009-0475-4

ORIGINAL PAPER

3D pharmacophore models for thromboxane A_2 receptor antagonists

Jing Wei · Yixi Liu · Songqing Wang

Received: 17 September 2008 / Accepted: 20 January 2009 / Published online: 5 March 2009

Abstract Thromboxane A_2 (TXA_2) is an endogenous arachidonic acid derivative closely correlated to thrombosis and other cardiovascular diseases. The action of TXA_2 can be effectively inhibited with TXA_2 receptor antagonists (TXRAs). Previous studies have attempted to describe the interactions between the TXA_2 receptor and its ligands, but their conclusions are still controversial. In this study, ligand-based computational drug design is used as a new and effective way to investigate the structure-activity relationship of TXRAs. Three-dimensional pharmacophore models of TXRAs were built with HypoGenRefine and HipHop modules in CATALYST software. The optimal HypoGenRefine model was developed on the basis of 25 TXRAs. It consists of two hydrophobic groups, one aromatic ring, one hydrogen-bond acceptor and four excluded volumes. The optimal HipHop model contains two hydrophobic groups and two hydrogen-bond acceptors. These models describe the key structure-activity relationship of TXRAs, can predict their activities, and can thus be used to design novel antagonists.

Keywords Thromboxane · Receptor · Antagonist · Pharmacophore model · HypoGen · HipHop

Electronic supplementary material The online version of this article (doi:10.1007/s00894-009-0475-4) contains supplementary material, which is available to authorized users.

J. Wei · Y. Liu · S. Wang (✉)
Tianjin Key Laboratory for Modern Drug Delivery & High-Efficiency, School of Pharmaceutical Science and Technology, Tianjin University,
92 Weijin Road, Nankai District,
Tianjin 300072, PR China
e-mail: wangsqphd@yahoo.com.cn

Introduction

Thromboxane A_2 (TXA_2) is an unstable metabolite of endogenous arachidonic acid. It is synthesized through the sequential actions of cyclooxygenases and thromboxane synthase in platelets, macrophages and lung parenchyma. It promotes the aggregation of platelets and constricts both vascular and bronchial smooth muscle [1, 2] through activation of its specific G-protein-coupled receptor, known as the TXA_2 receptor. Research on TXA_2 shows that it is closely correlated with various kinds of pathologies, including arterial and venous thrombosis [3] and renal and pulmonary diseases [4]. Inhibiting either the activity or the generation of TXA_2 should be an effective way to treat these disorders. Both TXA_2 synthase inhibitors and TXA_2 receptor antagonists (TXRAs) have been developed [5, 6] for this purpose. TXRAs have been shown to have potential therapeutic uses. However, TXA_2 synthase inhibitors do not show clinical efficacy due to the accumulation of prostaglandine H_2 (PGH_2, which is a precursor of TXA_2, and an agonist of the thromboxane receptor) [7].

Potent TXRAs with various structures have been developed during the past decades [8]. They can be classified into two main chemical groups: (1) prostanoid derivatives like nitrobenzenesulfonyl [9], 4-methyl-3,5-dioxanes [10], benzofurans [11] and benzo[1,4]oxazine [12]; and (2) non-prostanoid derivatives like bicyclo[3.1.0] hexanes [13], dibenzoxepins [14, 15] and oximes [16]. Several TXRAs can inhibit the platelet TXA_2 receptor at low nanomolar concentrations.

Point mutations have been performed on the TXA_2 receptor [17, 18]. Funk's group performed binding studies with SQ29, 548 (a TXRA) [17], which showed that the third intracellular loop of human TXA_2 receptor can be immunized, whereas the seventh transmembrane segment

cannot. Joseph et al. [18] reported that the Cys^{183}-Asp^{193} amino acid region in the C-terminal end of the third extracellular domain is critical for radioligand binding and platelet aggregation, while the Gly^{172}-Cys^{183} region in the N-terminal end is not.

Besides screening for active residues, some studies looked for essential ligand pharmacophores. Michaux's group [19] built a pharmacophore model for TXARs, which they applied to evaluate their newly synthesized antagonists. This was a qualitative model based on compounds with sulfonylurea structures.

The work presented here focused on the generation of three dimensional (3D) pharmacophore models for TXRAs using both HypoGenRefine and HipHop modules (quantitative and qualitative approaches) in the CATALYST software package [20]. The HypoGenRefine module is an improvement of the HypoGen module by the addition of excluded volumes, which represent incompatible steric clashes with the target. Our two models were both tested on a large set of structurally diverse TXRAs. The HypoGenRefine model was derived from the set of training molecules, which consisted of 25 TXRAs with known activity values. Additionally, seven other highly active TXRAs with various structures were used to formulate the HipHop hypotheses. The pharmacophore models can be used to predict the interaction between ligands and the TXA_2 receptor, and to identify specific TXRAs.

Materials and methods

All computations for the generation of pharmacophore models were performed with CATALYST 4.11 on an IBM6223I2C workstation.

We collected a series of TXRAs to generate pharmacophore models on the basis of their activity levels and structures. Twenty-five TXRAs (**1**–**25**, Fig. 1) with a dibenzoxepin skeleton were selected as the training set for HypoGenRefine models. Their activities ranged from 0.91 nM to 14,000 nM. Seven highly active TXRAs (compounds **26**–**32**) with various structures were used to formulate the HipHop hypotheses. Their structures and activities are shown in Fig. 2.

To validate the pharmacophore models obtained, we selected 30 TXRAs (compounds **33**–**62**, Fig. S1) to form the test set for the HypoGenRefine model, and 12 compounds (compounds **63**–**74**, Fig. S2) for the HipHop model.

All structures were built using a 2D/3D editor-sketcher and were minimized to a local energy minimum using the CHARMM-like force field. Since molecules might adjust their conformations when binding to a receptor, conformational models consisting of a representative set of conformers were generated to increase their flexibility. The BEST quality conformational search option was applied to each molecule, and implemented using the Poling algorithm

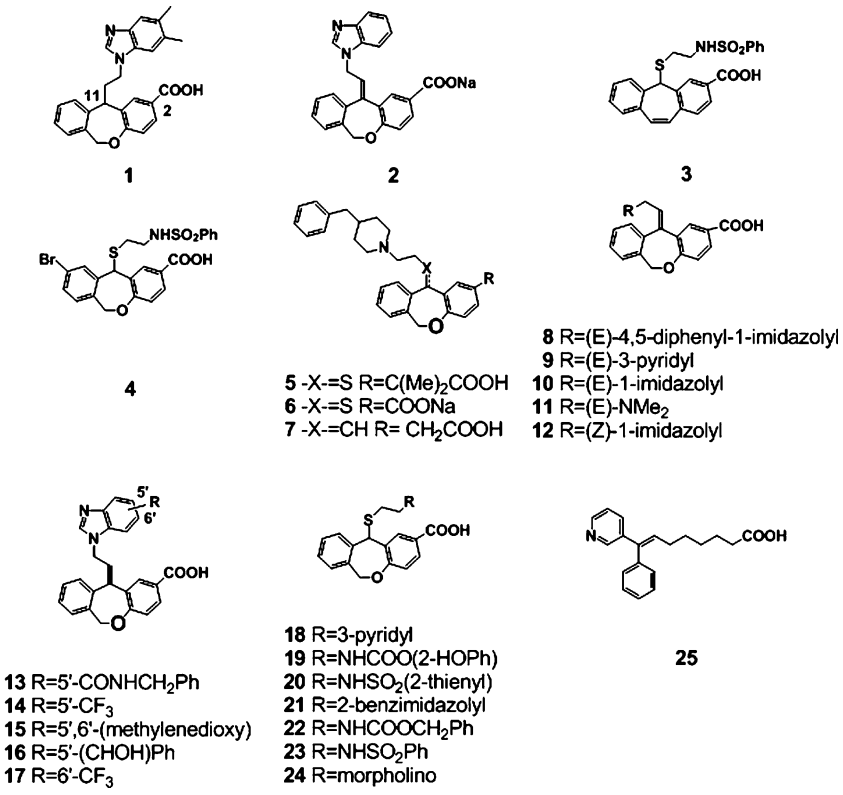

Fig. 1 Chemical structures of compounds **1**–**25** in the HypoGenRefin training set

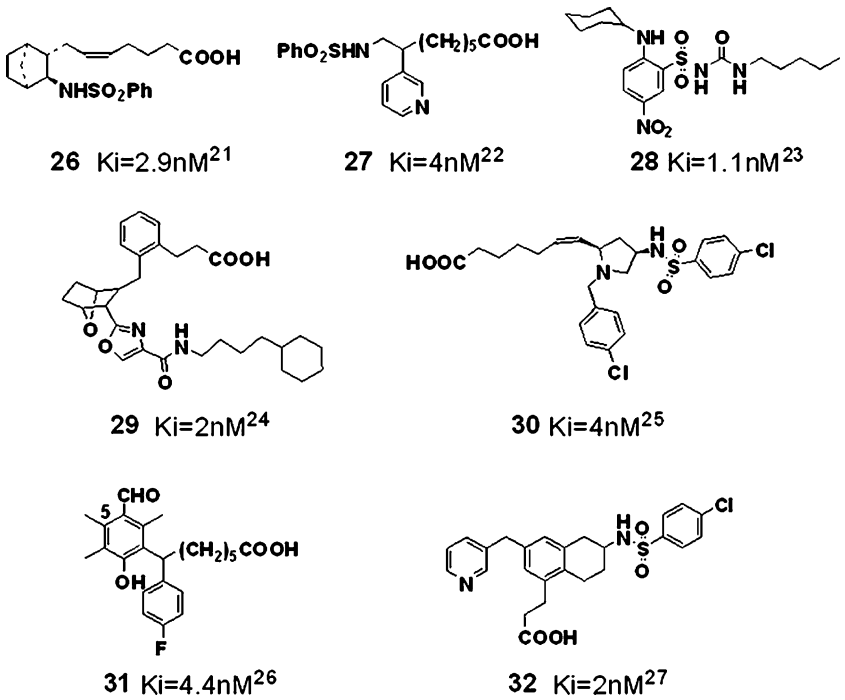

Fig. 2 Structures and activities of compounds **26**–**32** in the HipHop training set

[21]. The maximum number of conformers was set to 250. A relative conformational energy of 15 kcal mol^{-1} was chosen as conformation selection criterion.

Drawing on the characteristic features of the training-set molecules, aromatic ring (RA), hydrophobic (H) and hydrogen bond acceptor (HBA) were selected from the feature dictionary of CATALYST to form the essential basis for the hypothesis generation process.

Automatic hypothesis generation returned ten pharmacophore models with top ranking scores. These models were then evaluated and validated against the training and test sets.

Results and discussion

HypoGenRefine model

A set of ten hypotheses were generated automatically on the basis of the activities and structures of the 25 training compounds. The best pharmacophore hypothesis, named Hypo-1, was marked by the best correlation coefficient (0.91) and the highest cost difference (52.22). The parameters of Hypo-1 suggested that there was a more than 80% probability of accurately predicting the activities of the training set compounds, and thus evaluate effectively the quality of the pharmacophore hypothesis.

Hypo-1 included one HBA, one RA, two Hs and four excluded volumes (EV), labeled HBA, RA, H1, H2 and EV1–EV4. EV1 and EV2 were located around the H1 feature, while EV3 and EV4 were situated close to the H2 and RA features, respectively. The HBA, RA and H2 features were almost aligned, with an angle between them of about 160 degrees. A representation of the Hypo-1 hypothesis and the distances between its features is shown in Fig. S3.

All compounds were categorized according to their activities, as highly active (<10 nM, +++), moderately active (10–1,000 nM, ++), or inactive (>1,000 nM, +). All but three of the training set compounds were correctly predicted, one highly active molecule and one inactive molecule were erroneously predicted as moderately active, and one moderately active molecule was predicted to be highly active. The actual activities, estimated activities, activity scale and error values of all training-set compounds are listed in Table 1. The error value is defined as the ratio of estimated activity to measured activity if that ratio is greater than 1 (or as the ratio of measured activity to estimated activity, in which case the error value is negative).

A test set of 30 TXRAs (17 dibenzoxepin and 13 oxime derivatives) was analyzed in order to check the predictive power of the Hypo-1 hypothesis. The predicted activities of all compounds were confirmed, except for two moderately active compounds that were overpredicted (see Table S1). Altogether, the predicted K_i values of 91% of all compounds in the training and test sets were found to be within the same order of magnitude as the actual activities. Hypo-1 was regressed using each molecule in the training and test sets. The regression line shown in Fig. S4 indicates a good correlation between measured and estimated activities. All the facts above strongly confirm the

Table 1 Experimental biological data and estimated K_i of compounds of the training set, based on the Hypo-1 model

Compound no.	Reference	ActualK_i [nM]	Estimated K_i [nM]	Error	Activity scale[a]	Estimated scale[a]
13	[15]	0.91	1.0	+1.1	+++	+++
14	[15]	2.2	4.3	+2.0	+++	+++
15	[15]	2.7	9.1	+3.4	+++	+++
19	[14]	5.1	4.9	−1.0	+++	+++
20	[14]	5.7	25	+4.4	+++	++
16	[15]	6.1	1.6	−3.8	+++	+++
4	[14]	6.8	7.4	+1.1	+++	+++
21	[15]	7.6	6.9	−1.1	+++	+++
22	[14]	7.7	1.9	−4.1	+++	+++
2	[18]	15	6.9	−2.2	++	+++
1	[15]	18	24	+1.3	++	++
3	[14]	25	11	−2.3	++	++
23	[18]	32	33	+1.0	++	++
17	[15]	60	13	−4.6	++	++
8	[15]	164	110	−1.5	++	++
9	[19]	180	110	−1.6	++	++
10	[19]	600	470	−1.3	++	++
7	[18]	740	750	+1.0	++	++
11	[18]	1,000	890	−1.1	++	++
5	[18]	1,600	1,200	−1.3	+	+
24	[18]	1,900	1,500	−1.3	+	+
25	[19]	2,700	6,300	+2.3	+	+
12	[19]	4,500	440	−10.2	+	++
18	[19]	8,200	1,400	−5.9	+	+
6	[18]	14,000	1,200	−11.7	+	+

[a] Activity scale: highly active (<10 nM, +++), moderately active (10–1,000 nM, ++), or inactive (>1,000 nM, +)

reliability of our model to predict the activity of compounds.

The mapping analyses suggested that the Hypo-1 model mapped with the dibenzoxepin derivatives in a similar way (Fig. 3a). The HBA feature was occupied by the oxygen atom of the 2-carboxylic group on the dibenzoxepin ring. The H1 feature mapped onto the terminal benzene ring (or the heterocyclic middle group) at the 11-position side chain. Each of the H2 and RA features was characterized by a phenyl ring on the dibenzoxepin core structure.

The analyses suggested that the low 1,000 nM activity of some compounds can be explained by their imperfect mapping of the H1 feature in Hypo-1 at the level of the 11-side chain on the dibenzoxepin ring. For example, in compound **11**, the terminal methyl group on the 11-side chain proved to be too short to reach the H1 region. Regarding inactive compounds, the piperidine ring in the long sulfonamide chain in compounds **5** and **6** was inhibited by EV1 and EV2, therefore preventing mapping of the H1 feature (Fig. S5). These facts confirm that the presence of the H1 feature is essential to high affinity, and that the EV1 and EV2 surrounding it effectively restrict hydrophobic interactions between ligands and H1.

With oxime derivatives, the HBA feature was occupied by the oxygen atom of their carboxylic group. The H1 and H2 features mapped with their 1-phenyl ring (or 1-cyclohexyl ring) and 3-benzyl group, respectively. The RA region interacted with their 2-imidazolyl group (Fig. 3b). Compound **55** mapped with the H2 feature in Hypo-1, but compound **58**, which has a hydrogen atom instead of the 3-benzyl group in **55**, could not. This explained why there was a dramatic decrease in affinity from 80 to 27,300 nM. The general trend was a marked drop in affinity when a functional group that can map with the H2 feature was absent.

HipHop model

Ten hypotheses were returned according to their ranking scores. After validation of the training and test sets, the best model was singled out and renamed Hypo-2. It contained two HBA and two H features. To distinguish them from the

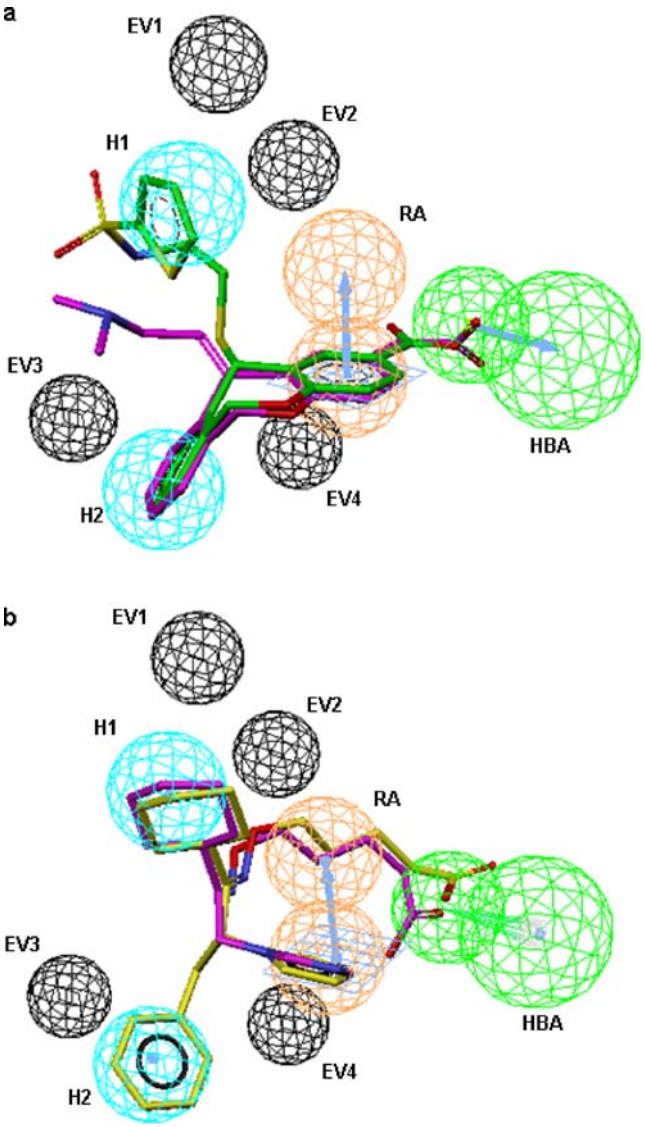

Fig. 3a,b Overlapping of thromboxane A_2 receptor antagonists (TXRAs) with Hypo-1 model. **a 11** (*purple*) and **20** (*green*). **b 55** (*yellow*) and **58** (*purple*). Spheres: *Green* Hydrogen bond acceptors (*HBA*), *cyan*hydrophobic (*H*), *orange* aromatic rings (*RA*), *black* excluded volumes (*EV*)

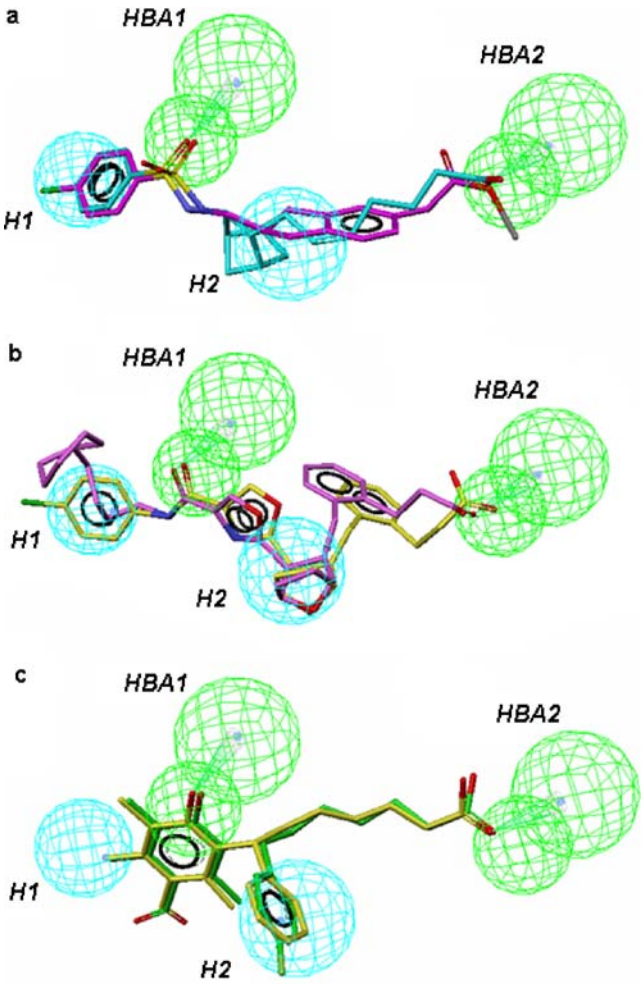

Fig. 4 Hypo-2 model mapped with some of the compounds. **a 26** (*light blue*) and **69** (*purple*). **b 29** (*purple*) and **65** (*yellow*), **c 31** (*green*) and **64** (*yellow*). Color coding of pharmacophore features as in Fig. 3

features of Hypo-1, they were marked in italics (*HBA1*, *HBA2*, *H1* and *H2*). Figure S6 illustrates the hypothesis and the distances between the features of Hypo-2.

The compounds used for the HipHop module belonged to various structural classes and mapped with four features of Hypo-2 (Table S2). The analysis of mapping situations showed that the HipHop model was able to successfully identify the crucial features common to all highly potent TXRAs. Figure 4 illustrates some mapping alignments of the chemical functional groups in different ways.

The benzene sulfonamide derivatives were fitted into the model in a similar orientation (Fig. 4a). For **26**, *HBA1* was represented by the oxygen atom of the sulfonyl group on the side chain, the *HBA2* region interacted with the oxygen atom of the terminal carboxylic group, *H1* was occupied by the phenyl ring of the sulfonylamino side chain, and *H2* interacted with the bicycle[2.2.1]heptane ring. The only difference was that *H2* matched various core rings, such as a 2,3-dihydro-indene in **63** and a tetrahydronaphthalene in **32** and **73**.

The phenyl ring (or naphthyl ring) on the side chain of 3-pyridinyl-substituted arylsulfonamido alkanoic acids (**27** and **68**) interacted with the *H1* region. The *H2* feature was occupied by the pyridine ring, and the *HBA1* and *HBA2* features were occupied by the oxygen atom of the sulfonyl group and by the carboxylic group, respectively (Fig. S7).

For 7-oxabicyclo[2.2.1]heptane oxazoles **29** and **65** (Fig. 4b), the *H1* feature was occupied by the aliphatic group or phenyl ring, the *H2* feature interacted with 7-oxabicyclo[2.2.1]heptane, the *HBA1* feature was occupied by the nitrogen atom of the amino group on the oxazole

side chain, and the *HBA2* region interacted with the oxygen atom of the carboxylic group on the phenylpropionic acid side chain. Joseph's group [18] found that the third transmembrane domain (TM3) coordinated with the prostanoid ring (oxabicyclo[2.2.1]heptane) of the compounds in this class, thus the *H2* feature in Hypo-2 might correspond to the TM3 of the receptor.

For phenol derivatives (**31** and **64**), their 5-methyl group mapped with the *H1* feature. The fluorobenzene ring mapped to the *H2* feature. The oxygen atom of the phenolic hydroxy group occupied the *HBA1* region. The oxygen atom of the carboxylic group matched the *HBA2* feature (Fig. 4c).

With benzofurans and benzo[1,4]oxazine derivatives **70** and **71** (Fig. S8), the H1 feature was occupied by the terminal phenyl ring linking the sulfur atom, the HBA1 feature interacted with the sulfur atom, the HBA2 feature interacted with the oxygen atom of the carboxylic group, and the H2 feature was occupied by the phenyl rings in the benzofuran group in **70**, and in the benzo[1,4]oxazine group in **71**, respectively.

With sulfonylurea derivatives **28** and **72**, the *H1* feature was occupied by the terminal alkyl group. The *H2* feature interacted with the cyclohexanyl (**28**) or phenyl ring (**72**) on the side chain. *HBA1* and *HBA2* were mapped by the oxygen atom in the sulfonylurea and by the nitric oxygen atom on the benzene ring, respectively (Fig. S9).

With compound **74** (Fig. S10), the *H1* feature mapped with the long alkyl chain grafted on the amino group, the *H2* feature mapped with the phenyl ring, the *HBA1* feature interacted with the carbonyl oxygen atom grafted on the amino group, and the *HBA2* feature was occupied by the carboxyl oxygen atom.

Michaux's group [19] also studied TXRAs by means of the HipHop approach of CATALYST. Their model included five features. To distinguish those features from those of Hypo-2, we renamed them as H', HBA1', HBA2', R' and N' (negative ionable). Michaux's group mapped compounds **28**, **73** and **74** onto their model too. Our comparison showed that the H' feature in their model corresponds to *H1* in Hypo-2, and interacts with the same positions in compounds **28**, **73** and **74**. Although the four other features in their model were not exactly the same as in Hypo-2, functional groups that occupied those features could almost map with the features in our model. When mapping with compounds **73** and **74**, the R' and N' features matched our *H2* and *HBA2* features, respectively, and mapped with the same functional groups in the two compounds. When mapping with compound **28**, the HBA2' feature played the same role as *HBA2*, which was occupied by the nitric oxygen atom, while R' was similar to the *H2* feature that could map with cyclohexanyl. Therefore, our observations were in agreement with Michaux's research. Our conclusion that the four features in Hypo-2 are all crucial for high activity antagonists is similar to their conclusion that the H', HBA1', R' and N' features are essential for high activity.

Conclusions

Two specific 3D pharmacophore hypotheses for TXRAs were studied through a ligand-based computational approach. Our quantitative model (Hypo-1) contains four chemical features and four excluded volumes. The four excluded volumes restrict the conformations of the compounds. The H1 feature, as well as the EV1 and EV2, play an important role in high binding affinity for the receptor. The Hypo-1 model is capable of predicting the activities of a wide range of TXRAs. The quantitative model (Hypo-2) contains two hydrophobic groups and two hydrogen bond acceptors. All chemical features of Hypo-2 seem to be essential to high antagonist potency.

These two pharmacophore models could be of great interest, not only to gain insight into the structure-activity relationships of these compounds, but also to clarify the specific roles of the TXA_2 receptor. The models could be used to screen compounds with various structures in search of potent antagonist activity.

Acknowledgments With special thanks to Dr. Kang Zhao, Mr. Philippe Andre, Dr. Chuanjie Wu and Mr. Peng Li for their dedicated support of this study.

References

1. Arita H, Nakano T, Hanasaki K (1989) Thromboxane Ap: its generation and role in platelet activation. Prog Lipid Res 28:273–301
2. Svensson J, Strandberg K, Tuvemo T et al (1977) Thromboxane A2: effects on airway and vascular smooth muscle. Prostaglandins 14:425–436
3. Schumacher WA, Heran CL, Steinbacher TE et al (1993) Superior activity of a thromboxane receptor antagonist as compared with aspirin in rat models of arterial and venous thrombosis. J Cardiovasc Pharmacol 22:526–533
4. Halushka PV, Allan CJ, Davis-Bruno KL (1995) Thromboxane A2 receptors. J Lipid Mediat Cell Signal 12:361–378
5. Collington EW, Finch H (1990) Thromboxane synthase inhibitors and receptor antagonists. Annu Rep Med Chem 25:99–108
6. Gresele P, Deckmyn H, Nenci GG et al (1991) Thromboxane synthase inhibitors, thromboxane receptor antagonists and dual blockers in thrombotic disorders. Trends Pharmacol Sci 12:158–163
7. Gresele P, Van Houtte E, Arnout J et al (1984) Thromboxane synthase inhibition combined with thromboxane receptor blockade: a step forward in antithrombotic strategy. Thromb Haemost 52:364
8. Hall SE (1991) Thromboxane A2 receptor antagonists. Med Res Rev 11:503–579
9. Hanson J, Dogné JM, Ghiotto J et al (2007) Design, synthesis, and SAR study of a series of N-alkyl-N′-[2-(aryloxy)-5-nitro-

benzenesulfonyl]ureas and-cyanoguanidine as selective antagonists of the TPα and TPβ isoforms of the human thromboxane A2 receptor. J Med Chem 50:3928–3936
10. Marusawa H, Setoi H, Kuroda A et al (1999) Synthesis and biological activity of 4-methyl-3,5-dioxane derivatives as thromboxane A2 receptor antagonists. Bioorg Med Chem 7:2635–2645
11. Ohno M, Miyamoto M, Hoshi K et al (2005) Development of dual-acting benzofurans for thromboxane A2 receptor antagonist and prostacyclin receptor agonist: synthesis, structure-activity relationship, and evaluation of benzofuran derivatives. J Med Chem 48:5279–5294
12. Ohno M, Tanaka Y, Miyamoto M et al (2006) Development of 3,4-dihydro-2 H-benzo[1,4]oxazine derivatives as dual thromboxane A_2 receptor antagonists and prostacyclin receptor agonists. Bioorg Med Chem 14:2005–2021
13. Kamata S, Haga N, Tsuri T et al (1990) Synthesis of thromboxane receptor antagonists with bicyclo[3.l.O]hexane ring systems. J Med Chem 33:229–239
14. Ohshima E, Takami H, Sato H et al (1992) Non-prostanoid thromboxane A2 receptor antagonists with a dibenzoxepin ring system. 1. J Med Chem 35:3394–3402
15. Ohshima E, Takami H, Sato H et al (1992) Non-prostanoid thromboxane A2 receptor antagonists with a dibenzoxepin ring system. 2. J Med Chem 35:3402–3413
16. Cozzi P, Giordani A, Menichincheri M et al (1994) Agents combining thromboxane receptor antagonism with thromboxane synthase inhibition: [[[2-(1 H-imidazol-1-yl)ethylidene]amino] oxy]alkanoic acids. J Med Chem 37:3588–3604
17. Funk CD, Furci L, Moran N et al (1993) Point mutation in the seventh hydrophobic domain of the human thromboxane A2 receptor allows discrimination between agonist and antagonist binding sites. Mol Pharmacol 44:934–939
18. Turek WJ, Halmos T, Sullivan LN et al (2002) Mapping of a ligand-binding site for the human thromboxane A2 receptor protein. J Biol Chem 277:16791–16797
19. Michaux C, Dogné JM, Rolin S (2003) A pharmacophore model for sulphonyl-urea (-cyanoguanidine) compounds with dual action, thromboxane receptor antagonists and thromboxane synthase inhibitors. Eur J Med Chem 38:703–710
20. CATALYST 4.11, Accelrys, San Diego, CA, USA, 2006
21. Smellie A, Teig SL, Towbin P (1995) Poling: promoting conformational variation. J Comput Chem 16:171–187